

21. Khaykovich, B. *et al.* Vortex-lattice phase transitions in  $\text{Bi}_2\text{Sr}_2\text{CaCu}_2\text{O}_8$  crystals with different oxygen stoichiometry. *Phys. Rev. Lett.* **76**, 2555–2558 (1996).
22. Cubitt, R. *et al.* Direct observation of magnetic flux lattice melting and decomposition in the high- $T_c$  superconductor  $\text{Bi}_{2.15}\text{Sr}_{1.95}\text{CaCu}_2\text{O}_{8+x}$ . *Nature* **365**, 407–411 (1993).
23. Deligiannis, K. *et al.* New features in the vortex phase diagram of  $\text{YBa}_2\text{Ca}_3\text{O}_{7-\delta}$ . *Phys. Rev. Lett.* **79**, 2121–2124 (1997).
24. Sullivan, P. F. & Seidel, G. Steady-state, ac-temperature calorimetry. *Phys. Rev.* **173**, 679–685 (1968).
25. Reichhardt, C., van Otterlo, A. & Zimányi, G. T. Vortices freeze like window glass: the vortex molasses scenario. *Phys. Rev. Lett.* **84**, 1994–1997 (2000).
26. Williams, G. A. Vortex-loop phase transitions in liquid helium, cosmic strings, and high- $T_c$  superconductors. *Phys. Rev. Lett.* **82**, 1201–1204 (1999).
27. Onsager, L. Statistical hydrodynamics. *Nuovo Cimento Suppl.* **6**, 279–287 (1949).

**Acknowledgements**

The measurements above 18 T were performed in the Grenoble High Magnetic Field Laboratory. Work at Argonne and Berkeley was supported by the US DOE.

Correspondence and requests for materials should be addressed to F.B. (e-mail: Frederic\_Bouquet@Yahoo.Com).immuno

.....  
**‘Inverse’ melting of a vortex lattice**

**Nurit Avraham\***, **Boris Khaykovich\*†**, **Yuri Myasoedov\***, **Michael Rappaport\***, **Hadas Shtrikman\***, **Dima E. Feldman\*‡**, **Tsuyoshi Tamegai§**, **Peter H. Kes||**, **Ming Li||**, **Marcin Konczykowski¶**, **Kees van der Beek¶** & **Eli Zeldov\***

\* Department of Condensed Matter Physics, The Weizmann Institute of Science, Rehovot 76100, Israel

‡ Landau Institute for Theoretical Physics, 142432 Chernogolovka, Moscow region, Russia

§ Department of Applied Physics, The University of Tokyo, Hongo, Bunkyo-ku, Tokyo 113-8656, and CREST, Japan Science and Technology Corporation (JST), Japan

|| Kamerlingh Onnes Laboratory, Leiden University, PO Box 9504, 2300 RA Leiden, The Netherlands

¶ Laboratoire des Solides Irradiés, CNRS, UMR 7642 and CEA/DSM/DRECAM, Ecole Polytechnique, 91128 Palaiseau, France

Inverse melting is the process in which a crystal reversibly transforms into a liquid or amorphous phase when its temperature is decreased. Such a process is considered to be very rare<sup>1</sup>, and the search for it is often hampered by the formation of non-equilibrium states or intermediate phases<sup>2</sup>. Here we report the discovery of first-order inverse melting of the lattice formed by magnetic flux lines in a high-temperature superconductor. At low temperatures, disorder in the material pins the vortices, preventing the observation of their equilibrium properties and therefore the determination of whether a phase transition occurs. But by using a technique<sup>3</sup> to ‘dither’ the vortices, we were able to equilibrate the lattice, which enabled us to obtain direct thermodynamic evidence of inverse melting of the ordered lattice into a disordered vortex phase as the temperature is decreased. The ordered lattice has larger entropy than the low-temperature disordered phase. The mechanism of the first-order phase transition changes gradually from thermally induced melting at high temperatures to a disorder-induced transition at low temperatures.

Local magnetization measurements, using microscopic Hall sensors<sup>4</sup>, were performed on a number of high-quality optimally doped  $\text{Bi}_2\text{Sr}_2\text{CaCu}_2\text{O}_8$  (BSCCO) crystals, grown in two laboratories<sup>5,6</sup>. A d.c. magnetic field  $H_a$  was applied parallel to the crystalline  $c$  axis, while an a.c. transverse field  $H_{ac\perp}$  was applied along the  $a$ – $b$  planes (see Fig. 1 legend for details).

In  $\text{YBa}_2\text{Cu}_3\text{O}_7$  at temperatures close to  $T_c$ , ‘vortex dithering’ by a transverse a.c. field reduces the irreversible magnetization caused by vortex pinning<sup>3</sup>. We find that in BSCCO crystals this method can fully suppress the magnetic hysteresis even at low temperatures, down to about 30 K, as shown in Fig. 1a. The Abrikosov vortices in BSCCO can be regarded as a stack of Josephson-coupled pancake vortices<sup>7</sup> in the individual  $\text{CuO}_2$  planes. The in-plane field  $H_{ac\perp}$  readily penetrates through the sample<sup>8</sup> in the form of Josephson vortices residing between the  $\text{CuO}_2$  planes<sup>9</sup>. The main effect, which is of interest here, is that a pancake vortex, located in a  $\text{CuO}_2$  plane immediately above a Josephson vortex, is displaced a small distance

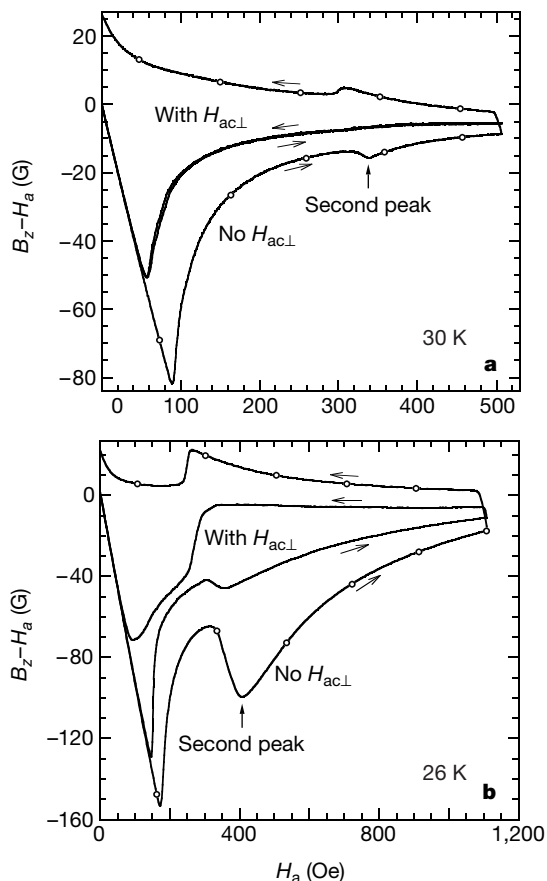


**Figure 1** Local magnetization loops in BSCCO crystals with and without (open circles) ‘vortex dithering’. A number of optimally doped BSCCO crystals with  $T_c \approx 90$  K were investigated. We present here results on three crystals: A ( $160 \times 600 \times 25 \mu\text{m}^3$ ), B ( $170 \times 600 \times 20 \mu\text{m}^3$ ) and C ( $190 \times 900 \times 30 \mu\text{m}^3$ ). The samples were mounted on an array of  $10 \times 10 \mu\text{m}^2$  GaAs/AlGaAs Hall sensors. A d.c. magnetic field  $H_a$  was applied perpendicular to the surface of the sensors (parallel to the crystalline  $c$  axis). A transverse a.c. field  $H_{ac\perp}$  (1 kHz with amplitude of up to 80 Oe), applied parallel to the  $ab$  planes of the crystals, equilibrates the vortices by ‘dithering’ and suppresses the magnetic hysteresis. The Hall sensors are insensitive to the transverse field and measure only the d.c.  $c$ -axis component  $B_z$  of the local induction. **a**, Lowest temperature, 30 K, at which fully reversible magnetization in crystal A is attained for our maximum  $H_{ac\perp}$  of  $\sim 80$  Oe. The d.c. magnetization loop displays the second magnetization peak above 300 Oe, which is due to the enhanced vortex pinning in the disordered phase. Application of  $H_{ac\perp}$  results in a reversible magnetization curve that reveals a small step in magnetization (barely seen on this scale) at the original location of the second magnetization peak. **b**, Example of the local magnetization loop at a lower temperature (26 K) in crystal B. The d.c. loop shows large hysteresis and a pronounced second magnetization peak. The applied  $H_{ac\perp}$  is not sufficient to obtain reversible magnetization. The ‘dithering’ efficiency of  $H_{ac\perp}$  is significantly different in the two vortex phases: For the same width of the original d.c. loop, much stronger suppression of the hysteresis is observed in the ordered phase than in the disordered phase above the second magnetization peak.

† Present address: Department of Physics and CMSE, Massachusetts Institute of Technology, Cambridge, Massachusetts 02139, USA.

along the direction of the Josephson vortices relative to the neighbouring pancake vortex residing one CuO<sub>2</sub> layer underneath<sup>9</sup>. For small values of  $H_{ac\perp}$ , the probability of such a close proximity between a pancake vortex and a Josephson vortex is low. Thus, in our sample geometry, an average pancake vortex experiences only a few such periodic 'intersections' during one a.c. cycle; the duration of each intersection is less than 1% of the a.c. period.  $H_{ac\perp}$  therefore induces a weak local a.c. agitation of pancake vortices, which assists thermal activation in relaxing the irreversible magnetization and in approaching thermal equilibrium.

In addition to bulk pinning, a substantial part of the magnetic hysteresis in BSCCO crystals is caused by surface<sup>10</sup> and geometrical barriers<sup>11</sup>.  $H_{ac\perp}$  also efficiently suppresses this source of hysteresis. The Josephson vortices, which periodically cross the sample edges, instantaneously 'slice' the Abrikosov vortices into short segments or individual pancakes, thus apparently facilitating<sup>10</sup> vortex penetration through the surface and geometrical barriers. At lower temperatures the equilibration of vortices by  $H_{ac\perp}$  becomes progressively more difficult, as shown in Fig. 1b at  $T = 26$  K, where our maximum  $H_{ac\perp}$  is not sufficient to eliminate the hysteresis completely.

We now focus on the main topic of vortex-matter phase transitions. At elevated temperatures the vortex lattice undergoes a first-order melting transition<sup>4,8,12,13</sup>. The melting line  $B_m(T)$  apparently terminates at some critical point  $T_{CP}$ , below which a 'second magnetization peak' line  $B_{sp}(T)$  emerges<sup>14-17</sup>. In BSCCO crystals the  $B_{sp}(T)$  line is rather horizontal on the  $B-T$  phase diagram. On crossing this line by a field sweep, a pronounced 'second peak' is observed in magnetization loops<sup>14</sup> (Fig. 1), which reflects a transformation of a quasi-ordered lattice into a disordered amorphous state with enhanced vortex pinning.

The first-order nature of the melting transition  $B_m(T)$  is manifested by a small step in equilibrium magnetization, as described in Fig. 2. At high temperatures,  $H_{ac\perp}$  has no observable effect on this step. As the temperature is decreased along  $B_m(T)$  towards  $T_{CP}$ , magnetic hysteresis starts to set in gradually, as seen for example in Fig. 2a. Here, at  $T > T_{CP}$ , the magnetization step is still clearly resolved, but it is partly suppressed by the hysteresis in the vortex solid phase below the transition. Application of  $H_{ac\perp}$  fully removes the hysteresis and enhances the magnetization step.  $H_{ac\perp}$  also results in a small broadening of the transition. We attribute this broadening to the fact that a transverse field slightly decreases<sup>9</sup> the melting field  $B_m$ . The small variation of  $B_m$  during the a.c. cycle of  $H_{ac\perp}$  should therefore cause some smearing of the magnetization step.

Figure 2b shows the behaviour at  $T = 38$  K, just below  $T_{CP}$ , where the first-order transition was believed to be absent. At this temperature, significant hysteresis is observed and the second magnetization peak starts to develop. Application of  $H_{ac\perp}$  eliminates the hysteresis and instead a step in reversible magnetization emerges, which reveals the existence of a first-order transition. A similar phenomenon is found at lower temperatures, as shown in Fig. 2c, where a clear second magnetization peak turns into a step in magnetization upon application of  $H_{ac\perp}$  (see also Fig. 1a). This finding leads to several important conclusions, including the following: (1) the first-order transition does not terminate at  $T_{CP}$ , (2) the vortex matter displays inverse melting, (3) the underlying mechanism of the first-order transition is different above and below  $T_{CP}$ , and (4) the disorder-driven transition at the second magnetization peak is of first order.

(1) The first conclusion is that the previously reported termination of the first-order transition<sup>4</sup> at  $T_{CP}$  does not reflect a real critical point, but rather an experimental limitation. Below  $T_{CP}$  the dynamics becomes too slow to achieve vortex equilibration on typical experimental timescales, thus preventing observation of the equilibrium magnetization step.  $H_{ac\perp}$  accelerates the equilibration process<sup>3</sup> and thus facilitates the detection of the magnetization step down to significantly lower temperatures.

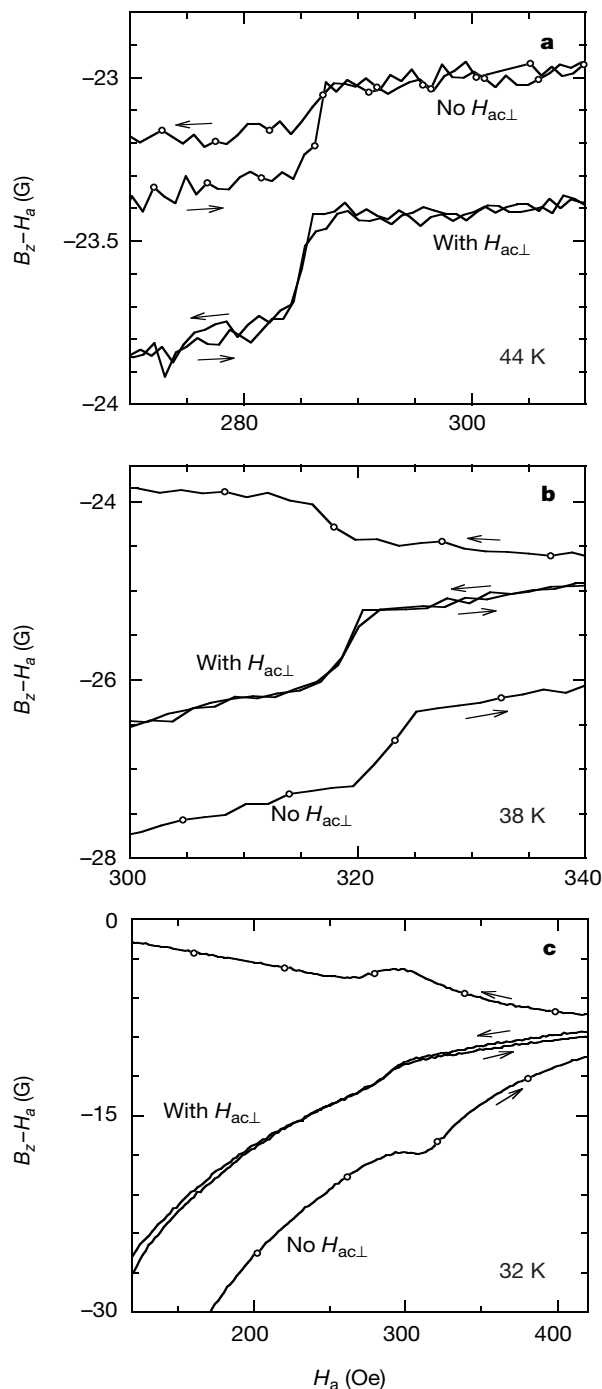


**Figure 2** Reversible magnetization steps revealed in BSCCO crystals by 'vortex dithering' at various temperatures. At high temperatures the first-order magnetization step occurs in the region of reversible magnetization. In this case  $H_{ac\perp}$  has no effect on the magnetization step up to our maximum transverse field of 80 Oe. In addition, there are no heating effects, as confirmed by the absence of a temperature shift in  $B_m(T)$ . **a**, At intermediate temperatures, such as  $T = 44$  K  $> T_{CP} \approx 40$  K (crystal C), hysteretic magnetization is observed below the transition (open circles). Application of  $H_{ac\perp}$  removes the residual hysteresis and enhances the magnetization step. Here the curve with  $H_{ac\perp}$  was displaced downwards for clarity. **b**, At temperatures slightly below  $T_{CP}$ , significant hysteresis develops in the d.c. magnetization loops and the beginning of the second-magnetization-peak behaviour is observed in the form of a pronounced change in the width of the loop.  $H_{ac\perp}$  results in reversible magnetization and reveals a clear magnetization step that appears instead of the second magnetization peak (crystal C,  $T = 38$  K). **c**, At still lower temperatures a fully developed second magnetization peak is observed in the d.c. magnetization loop which is replaced by a step in the reversible magnetization in the presence of  $H_{ac\perp}$  (crystal B,  $T = 32$  K).

(2) Observation of the magnetization step below  $T_{CP}$  is not simply an extension of the range of the first-order transition, but rather provides qualitatively new information. Figure 3 shows the location of the transition line on the  $B$ - $T$  phase diagram. Without  $H_{ac\perp}$ , the first-order transition is observed only at temperatures above  $T_{CP}$ , where  $B_m(T)$  has a negative slope  $dB_m/dT$ . We note that  $B_m(T)$  becomes horizontal<sup>4</sup> on approaching  $T_{CP}$ . By applying  $H_{ac\perp}$  we find that the first-order transition extends to significantly lower temperatures and shows an inverted behaviour of a positive slope below  $T_{CP}$ . Hence, in this region the vortex matter displays the very rare phenomenon of inverse melting in which an ordered lattice (Bragg glass<sup>18,19</sup>) reversibly transforms into a liquid or amorphous phase upon cooling.

(3) In a thermally driven vortex-melting transition, the liquid phase has to be on the high-temperature side of the transition because thermal fluctuations always increase with temperature. The observed inverse melting behaviour therefore implies that the first-order transition below  $T_{CP}$  must have a different underlying nature, which is disorder-driven rather than thermally driven. The main conceptual difference is that in thermal melting the decrease in elastic energy of the lattice at the transition is compensated for by a gain in entropy of the liquid. In a disorder-driven transition, in contrast, the loss of elastic energy is balanced by a gain in pinning energy, because the 'wiggling' entangled vortices adapt more efficiently to the pinning landscape induced by the quenched material disorder<sup>20</sup>. At low fields, the elastic energy of the lattice is higher than the pinning energy, giving rise to an ordered state<sup>18-20</sup>. With increasing field the elastic energy decreases relative to pinning, leading to a structural transformation into a disordered phase when the two energies become comparable. Our finding shows that this non-thermal transition is of first order. At low temperatures the shape of the disorder-driven transition line should be nearly temperature independent or may show downward curvature due to the temperature dependence of the microscopic parameters<sup>21</sup>. At intermediate temperatures, however, even though the transition remains disorder-driven, thermal smearing of the pinning potential progressively reduces the pinning energy, leading to an upturn in the transition line<sup>20</sup>. This effect of pinning reduction is apparently at

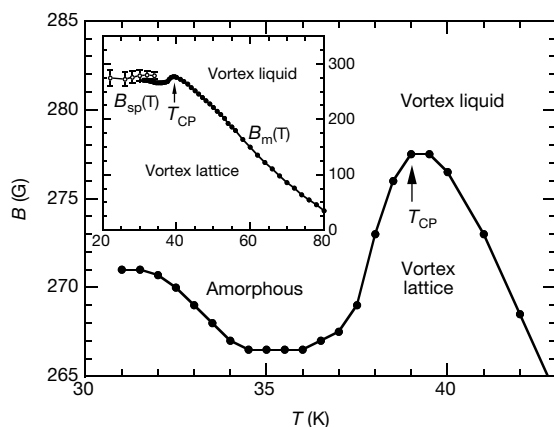


**Figure 3** The first-order transition line and the inverse melting obtained with 'vortex dithering'. Inset, the first-order  $B_m(T)$  line (filled circles) along with the second magnetization peak line  $B_{sp}(T)$  (open circles) over a wide temperature range in BSCCO crystal B.  $B_{sp}(T)$  was measured without  $H_{ac\perp}$  and the error bars reflect the uncertainty in the determination of the location of the  $B_{sp}$  transition owing to its larger width in comparison with the width of the first-order magnetization step. Main panel, an expanded view of the first-order transition line in the vicinity of  $T_{CP}$ . The first-order transition was observed at all temperatures at which fully reversible magnetization was achieved by 'vortex dithering'. At  $T < 31$  K no reversible magnetization could be attained in this crystal with our maximum  $H_{ac\perp}$  and hence no magnetization step could be revealed.

the origin of the observed inverse melting behaviour. An upturn in the shape of the second magnetization peak line has been noted previously<sup>5,14</sup>; however, the results presented here are, to our knowledge, the first evidence of a thermodynamic inverse melting transition of the vortex lattice.

(4) The extended  $B_m(T)$  transition line coincides with the location of the  $B_{sp}(T)$  line at lower temperatures, as seen in the inset to Fig. 3, which demonstrates that the two phenomena have a common origin. The second magnetization peak is the dynamic characteristic of the transition, reflecting the enhanced vortex pinning and the viscous nature of the disordered amorphous phase, whereas the reversible magnetization step is its thermodynamic signature. The revealed first-order nature of the second peak is consistent with recent conclusions based on Josephson plasma resonance studies<sup>22</sup> and transient measurements<sup>23,24</sup>, as well as several numerical simulations<sup>25-27</sup>. Thus, the breakdown of the Bragg glass is apparently always a first-order transition that occurs through a thermal and/or a disorder-driven mechanism. Whereas thermally driven melting is possibly restricted to high-temperature superconductors, the disorder-driven transition should be a more general phenomenon and is apparently at the heart of the ubiquitous peak effect in low- $T_c$  superconductors<sup>28</sup>.

Figure 4 shows the magnetization step  $\Delta B$  and the corresponding entropy change  $\Delta S = -(dH_m/dT)\Delta B/4\pi$  in the vicinity of  $T_{CP}$ .  $\Delta B$  is approximately constant in this region. The entropy change  $\Delta S$  vanishes at  $T_{CP}$  because  $dH_m/dT = 0$ , and becomes negative below  $T_{CP}$ . A negative  $\Delta S$  means that, paradoxically, the ordered lattice has larger entropy than the disordered phase. Because the ordered lattice has no dislocations and is structurally more ordered, the extra entropy must arise from additional degrees of freedom. In the amorphous phase the lattice structure is broken and the vortices wander out of their unit cells and become entangled, yet their thermal fluctuations on short timescales are small due to enhanced pinning. In contrast, in the ordered lattice there is no entanglement and no large-scale vortex wandering; however, thermal fluctuations within the unit cell are larger, apparently resulting in larger entropy.

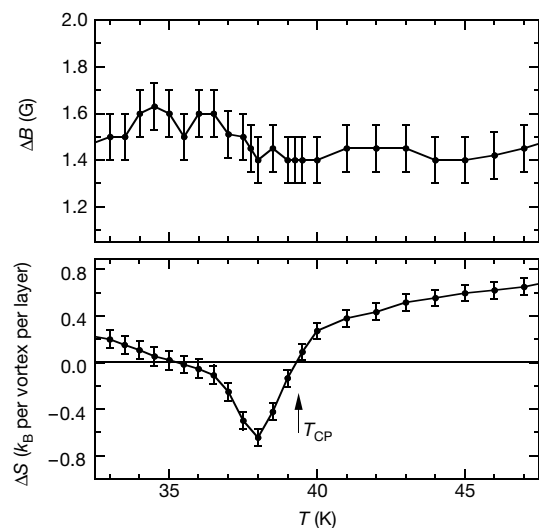


**Figure 4** Magnetization step and the negative latent heat. The top panel is the height of the magnetization step  $\Delta B$  in BSCCO crystal B in the vicinity of  $T_{CP}$  obtained in the presence of  $H_{ac\perp}$ . The bottom panel shows the corresponding calculated entropy change  $\Delta S$  (or the latent heat  $T\Delta S$ ). The negative  $\Delta S$  below  $T_{CP}$  is the region of the inverse melting transition of the vortex lattice. In this region, on increasing field, the melting of the lattice is accompanied by a negative latent heat. However, on crossing this transition line by increasing the temperature, the opposite process of crystallization of the amorphous phase occurs, which is accompanied by a positive latent heat.

$\Delta S < 0$  also means that the latent heat  $T_m \Delta S$  is negative, and hence the sample releases heat upon melting on increasing the field, in contrast to the usual melting in which the sample absorbs heat. Note, however, that by crossing the transition lines by increasing the temperature, the latent heat is always positive, as dictated by thermodynamics, and the high-temperature phase always has larger entropy. The observation of a rather constant  $\Delta B$  in Fig. 4 resolves another previously reported<sup>4</sup> inconsistency in the behaviour near  $T_{CP}$ : at a true critical point  $\Delta B$  is expected to vanish continuously, whereas experimentally a rather constant  $\Delta B$  was found to disappear abruptly at  $T_{CP}$ . The consistent values of  $\Delta B$  above and below  $T_{CP}$  clearly indicate a smooth continuation of the first-order transition and the absence of a real critical point. However, we emphasize that the vortex system may not be in full thermal equilibrium in the presence of  $H_{ac\perp}$  agitation. Therefore the relatively large values of  $\Delta B$  in Fig. 4, which are found to be sample dependent, should be investigated further.

Finally, an important open question is whether the two disordered states of the vortex matter, liquid and amorphous, represent different thermodynamic phases or just a continuous slowing down of vortex dynamics. Recent numerical calculations led to contradictory conclusions<sup>25–27,29</sup>. We do not observe any sharp features along the depinning line  $T_d$ , which usually extends upwards<sup>30</sup> from  $T_{CP}$  and is believed to separate the two phases. A strongly first-order  $T_d$  transition would require a sharp change in slope of  $B_m(T)$  at  $T_{CP}$ , which we do not observe. Therefore, the  $T_d$  line in BSCCO is unlikely to be a first-order transition; it could be either a continuous transition or a dynamic crossover. Similarly, in  $YBa_2Cu_3O_7$  the structure of the phase diagram is controversial, and it is as yet unclear whether the second magnetization peak line merges with the melting line at the critical point<sup>16</sup> or at a lower field. □

Received 4 January; accepted 21 March 2001.

- Greer, A. L. Too hot to melt. *Nature* **404**, 134–135 (2000).
- Rastogi, S., Höhne, G. W. H. & Keller, A. Unusual pressure-induced phase behaviour in crystalline poly(4-methylpentene-1): calorimetric and spectroscopic results and further implications. *Macromolecules* **32**, 8897–8909 (1999).
- Willemin, M. *et al.* First-order vortex-lattice melting transition in  $YBa_2Cu_3O_7$  near the critical temperature detected by magnetic torque. *Phys. Rev. Lett.* **81**, 4236–4239 (1998).
- Zeldov, E. *et al.* Thermodynamic observation of first-order vortex-lattice melting transition. *Nature* **375**, 373–376 (1995).
- Ooi, S., Shibauchi, T. & Tamegai, T. Evolution of vortex phase diagram with oxygen-doping in  $Bi_2Sr_2CaCu_2O_{8+\delta}$  single crystals. *Physica C* **302**, 339–345 (1998).
- T. W. Li *et al.* Growth of  $Bi_2Sr_2CaCu_2O_{8+\delta}$  single-crystals at different oxygen ambient pressures. *J. Cryst. Growth* **135**, 481–486 (1994).
- Blatter, G. *et al.* Vortices in high-temperature superconductors. *Rev. Mod. Phys.* **66**, 1125–1388 (1994).
- Pastoriza, H., Goffman, M. F., Arribere, A. & de la Cruz, F. First order phase transition at the irreversibility line of  $Bi_2Sr_2CaCu_2O_8$ . *Phys. Rev. Lett.* **72**, 2951–2954 (1994).
- Koshelev, A. E. Crossing lattices, vortex chains, and angular dependence of melting line in layered superconductors. *Phys. Rev. Lett.* **83**, 187–190 (1999).
- Burlachkov, L., Koshelev, A. E. & Vinokur, V. M. Transport properties of high-temperature superconductors: surface vs bulk effect. *Phys. Rev. B* **54** 6750–6757 (1996).
- Zeldov, E. *et al.* Geometrical barriers in high-temperature superconductors. *Phys. Rev. Lett.* **73**, 1428–1431 (1994).
- Safar, H. *et al.* Experimental evidence for a first-order vortex-lattice-melting transition in untwinned single crystal  $YBa_2Cu_3O_7$ . *Phys. Rev. Lett.* **69**, 824–827 (1992).
- Kwok, W. K. *et al.* Vortex lattice melting in untwinned and twinned single-crystals of  $YBa_2Cu_3O_{7-\delta}$ . *Phys. Rev. Lett.* **69**, 3370–3373 (1992).
- Khaykovich, B. *et al.* Vortex lattice phase transitions in  $Bi_2Sr_2CaCu_2O_8$  crystals with different oxygen stoichiometry. *Phys. Rev. Lett.* **76**, 2555–2558 (1996).
- Chikumoto, N., Konczykowski, M., Motohira, N. & Malozemoff, A. P. Flux-creep crossover and relaxation over surface barriers in  $Bi_2Sr_2CaCu_2O_8$  crystals. *Phys. Rev. Lett.* **69**, 1260–1263 (1992).
- Deligiannis, K. *et al.* New features in the vortex phase diagram of  $YBa_2Cu_3O_7$ . *Phys. Rev. Lett.* **79**, 2121–2124 (1997).
- Cubitt, R. *et al.* Direct observation of magnetic flux lattice melting and decomposition in the high- $T_c$  superconductor  $Bi_2Sr_2CaCu_2O_8$ . *Nature* **365**, 407–411 (1993).
- Giamarchi, T. & Le Doussal, P. Elastic theory of pinned flux lattice. *Phys. Rev. Lett.* **72**, 1530–1533 (1994).
- Nattermann, T. & Scheidl, S. Vortex-glass phases in type-II superconductors. *Adv. Phys.* **49**, 607–704 (2000).
- Ertas, D. & Nelson, D. R. Irreversibility, entanglement and thermal melting in superconducting vortex crystals with point impurities. *Physica C* **272**, 79–86 (1996).
- Giller, D. *et al.* Disorder-induced transition to entangled vortex-solid in Nd-Ce-Cu-O crystal. *Phys. Rev. Lett.* **79**, 2542–2545 (1997).
- Gaifullin, M. B. *et al.* Abrupt change of Josephson plasma frequency at the phase boundary of the

- Bragg glass in  $Bi_2Sr_2CaCu_2O_{8+\delta}$ . *Phys. Rev. Lett.* **84**, 2945–2948 (2000).
- van der Beek, C. J., Colson, S., Indenbom, M. V. & Konczykowski, M. Supercooling of the disordered vortex lattice in  $Bi_2Sr_2CaCu_2O_{8+\delta}$ . *Phys. Rev. Lett.* **84**, 4196–4199 (2000).
- Giller, D., Shaulov, A., Tamegai, T. & Yeshurun, Y. Transient vortex states in  $Bi_2Sr_2CaCu_2O_{8+\delta}$  crystals. *Phys. Rev. Lett.* **84**, 3698–3701 (2000).
- Kierfeld, J. & Vinokur, V. Dislocations and the critical endpoint of the melting line of vortex line lattices. *Phys. Rev. B* **61**, R14928–R14931 (2000).
- Nonomura, Y. & Hu, X. Effects of point defects on the phase diagram of vortex states in high- $T_c$  superconductors in  $Bllc$  axis. Preprint cond-mat/0011349 at (<http://xxx.lanl.gov>) (2000).
- Olsson, P. & Teitel, S. Disorder driven melting of the vortex line lattice. Preprint cond-mat/0012184 at (<http://xxx.lanl.gov>) (2000).
- Paltiel, Y. *et al.* Instabilities and disorder-driven first-order transition of the vortex lattice. *Phys. Rev. Lett.* **85**, 3712–3715 (2000).
- Reichhardt, C., van Otterlo, A. & Zimányi, G. T. Vortices freeze like window glass: the vortex molasses scenario. *Phys. Rev. Lett.* **84**, 1994–1997 (2000).
- Fuchs, D. T. *et al.* Possible new vortex matter phases in  $Bi_2Sr_2CaCu_2O_8$ . *Phys. Rev. Lett.* **80**, 4971–4974 (1998).

Acknowledgements

We thank V. B. Geshkenbein for valuable discussions. This work was supported by the Israel Science Foundation – Center of Excellence Program, by the Minerva Foundation, Germany, by the Mitchell Research Fund, and by a Grant-in-Aid for Scientific Research from the Ministry of Education, Science, Sports and Culture, Japan. D.E.F. acknowledges support from a Koshland Fellowship and an RFBR grant. P.K. and M.L. acknowledge support from the Dutch Foundation FOM. E.Z. acknowledges support from the Fundacion Antorchas – WIS program and from the Ministry of Science, Israel.

Correspondence and requests for materials should be addressed to N.A. (e-mail: nurit.avraham@weizmann.ac.il).

Coherent transfer of Cooper pairs by a movable grain

L. Y. Gorelik\*†, A. Isacson\*‡, Y. M. Galperin†‡, R. I. Shekhter\*‡ & M. Jonson\*‡

\* Department of Applied Physics, Chalmers University of Technology; and Göteborg University, SE-412 96 Göteborg, Sweden  
 † Department of Physics, University of Oslo, PO Box 1048, N-0316 Oslo, Norway; and Division of Solid State Physics, Ioffe Institute of the Russian Academy of Sciences, St Petersburg 194021, Russia  
 ‡ Centre for Advanced Study, Drammensveien 78, 0271 Oslo, Norway

Superconducting circuits that incorporate Josephson junctions are of considerable experimental and theoretical interest, particularly in the context of quantum computing<sup>1–5</sup>. A nanometre-sized superconducting grain (commonly referred to as a Cooper-pair box<sup>2</sup>) connected to a reservoir by a Josephson junction is an important example of such a system. Although the grain contains a large number of electrons, it has been experimentally demonstrated<sup>6</sup> that its states are given by a superposition of only two charge states (differing by  $2e$ , where  $e$  is the electronic charge). Coupling between charge transfer and mechanical motion in nanometre-sized structures has also received considerable attention<sup>7–10</sup>. Here we demonstrate theoretically that a movable Cooper-pair box oscillating periodically between two remote superconducting electrodes can serve as a mediator of Josephson coupling, leading to coherent transfer of Cooper pairs between the electrodes. Both the magnitude and the direction of the resulting Josephson current can be controlled by externally applied electrostatic fields.

First let us consider an isolated superconducting grain that is brought into direct contact with a bulk superconductor and then removed. Suppose that initially the grain was in a ground state  $|n\rangle$  with a fixed number of Cooper pairs  $n$ , counted from the neutral state, while the macroscopic lead, labelled  $b$ , was in a ground state